BJO Online First, published on August 26, 2011 as 10.1136/bjophthalmol-2011-300660

Development and validation of a computer-aided diagnostic tool to screen for age-related macular degeneration by optical coherence tomography

P Serrano-Aguilar,[1,2] R Abreu,[3] L Antón-Canalís,[4] C Guerra-Artal,[4] Y Ramallo-Fariña,[2,5] F Gómez-Ulla,[6] J Nadal[7]

► Additional material is published online only. To view this file please visit the journal online (http://bjo.bmj.com).

[1]Evaluation and Planning Unit, Canary Islands Health Service, Canary Islands, Spain
[2]CIBER Epidemiología y Salud Pública (CIBERESP), Barcelona, Spain
[3]Department of Ophthalmology, University Hospital of La Candelaria, Canary Islands, Spain
[4]Artificial Intelligence and Systems Group (GIAS), University of Las Palmas de Gran Canaria, Canary Islands, Spain
[5]Canary Islands Foundation for Health and Research (FUNCIS), Canary Islands, Spain
[6]Technological Institute of Ophthalmology (ITO), University of Santiago de Compostela, Santiago de Compostela, Spain
[7]Barraquer Ophthalmology Centre, Barcelona, Spain

Correspondence to
Dr Pedro Serrano-Aguilar, C/ Pérez de Rozas, n° 5, 4ª planta, CP: 38004, Santa Cruz de Tenerife, Islas Canarias, Spain; pserrano@gobiernodecanarias.org

Accepted 27 July 2011

ABSTRACT

Background To develop and assess the technical validity of new computer-aided diagnostic software (CAD) for automated analyses of optical coherence tomography (OCT) images for the purpose of screening for neovascular age-related macular degeneration.

Methods Artificial visual techniques were used to develop the CAD in two steps: normalisation and feature vector extraction from OCT images; and training and classification by means of decision trees. Technical validation was performed by a retrospective study design based on OCT images randomly extracted from clinical charts. Images were classified as normal or abnormal to serve for screening purposes. Sensitivity, specificity, positive predictive values and negative predictive values were obtained.

Results The CAD was able to quantify image information by working in the perceptually uniform hue—saturation—value colour space. Particle swarm optimisation with Haar-like features is suitable to reveal structural features in normal and abnormal OCT images. Decision trees were useful to characterise normal and abnormal images using feature vectors obtained from descriptive statistics of detected structures. The sensitivity of the CAD was 96% and the specificity 92%.

Conclusions This new CAD for automated analysis of OCT images offers adequate sensitivity and specificity to distinguish normal OCT images from those showing potential neovascular age-related macular degeneration. These results will enable its clinical validation and a subsequent cost-effectiveness assessment to be made before recommendations are made for population-screening purposes.

INTRODUCTION

Age-related macular degeneration (AMD) is the leading cause of visual impairment and blindness in industrialised nations among individuals of 65 years or older.[1] Up to now, there has been little reason to screen for AMD as there was insufficient evidence on treatment effectiveness for AMD. The recent advent of antioxidant and mineral supplementation to reduce AMD progression,[2] together with new treatment options for neovascular AMD (nAMD),[3] call for new research on the feasibility and cost-effectiveness of screening programmes,[4 5] with consideration of concomitant new advances in diagnostic and communications technologies.

There have some reports describing the technical validity and clinical utility of computer-aided diagnosis (CAD) technologies based on software development for automated image recognition.[6] These new tools have become one of the major research subjects in ophthalmologic diagnostic by imaging, complementing the clinical performance of doctors in interpreting retinal lesions in common health problems such as diabetic retinopathy[7] or AMD.[8] A considerable number of CAD systems have been developed to assist physicians in the early detection of complications of diabetic retinopathy, proving its technical validity with sensitivity and specificity values of about 90%,[7 9] coupled with the reduction in workload for doctors.[10]

Optical coherence tomography (OCT) is a non-invasive diagnostic technique involving analysis of optical interference patterns of cross-sectional images of the retina suitable for automated measurement and interpretation by means of CAD. Most existing research on the field has focused on the detection of retinal layer boundaries and measurement of layer thickness by a variety of means: random Markov fields, snake algorithms, Kalman filters and k-means.[11] Despite its descriptive contributions, no results have been published on abnormal images and potential clinical applications. Texture analyses have been used to segment inner and outer retinal layers by means of artificial neural networks. While it seems to work with abnormal images, it only detects two layers.[12] A basic edge detection kernel based on the first derivative of Gaussian in the vertical direction, supported by non-maxima suppression and hysteresis thresholding to detect edge points has been used to label up to six retinal layers.[13] A priori knowledge of edge polarity was applied to find each retinal layer without reporting on abnormal images. Support vector machines (SVM) were used in three-dimensional OCT images to perform semi-automatic segmentation and measurement of retinal layer thickness.[14] However, none of these previous experiences focused on classification of OCT images. Although automated detection of clinically significant macular oedema by grid-scanning OCT was developed by Sadda *et al*,[15] no studies have reported assessing the value of CAD to screen AMD using OCT images.

This pilot study was designed as a sequential proof of concept evaluation to determine the technical validity of new software for automated analyses of OCT images (optical coherence tomography automatic labeller (OCTAL)) for nAMD screening. OCTAL includes a complete analysis and classification system instead of focusing on the detection of retinal layers.

METHODS

CAD development

Artificial visual techniques[16–18] have been used to develop, successively, different versions of dedicated software in C++ for unassisted OCT image analysis and classification, consisting of two stages: (1) normalisation and feature vector extraction from OCT images; and (2) training and classification by means of decision trees.

Normalisation

In order to simplify operational conditions to the predefined image format settings of Zeiss Meditec OCT image capture systems, the current approach works with false colour red–green–blue (RGB) OCT images. This pre-processing stage both transforms colour images back to grey-scale values, representing reflectivity, and corrects image deformations. OCT false colours were first transformed to grey-level values applying a mapping function based on hue and brightness, preserving tissue reflectivity. Deformations and translations due to errors in the registration process were then modelled by fitting a single quadratic Bezier curve to the brightest tissue data points. Finally, OCT images were corrected by warping pixels to an ideal image where control points lay on a vertically centred horizontal line. This final image was smoothed with a median filter to remove high-frequency noise (figure 1).

Quantisation

Normalised images were processed to obtain the five most representative reflectivity levels.[19] This step allowed us to develop a background–foreground image mask (corresponding to tissue presence) and to obtain a first feature vector that contained the density of each reflectivity level. The computed mask was combined with normalised images to remove background noise. We did not take into account the retinal thickness in the analysis process due to the known variability with age.[20]

Feature vector extraction

Normalised and masked OCT images were then described using a feature vector that contained both the mean and SD of kurtosis and skewness of the structures detected on each A-scan, and the horizontal location and detected clivus correctness in the foveal region. Detected structures included the location of the inner limiting membrane, the location of the retinal pigment epithelium (RPE), and the location and local contrast of the darkest tissue region (which might correspond to a hole in the tissue). Values were normalised with respect to the image size to provide scale invariance of the feature vector. These structures are located using a particle swarm optimisation approach to optimise the functions that best describe each structure in terms of Haar-like features (figure 2).[16]

Training and classification

The C4.5 statistical classifier algorithm[17] as implemented in the data-mining software Weka[18] was used to build a decision tree from feature vectors extracted from 124 normal OCT images (healthy individuals) and 136 abnormal OCT images (AMD patients) (see online supplement). A k-fold cross-validation strategy[21] was applied to estimate the predictive value of the CAD when applied to novel images.

Technical validation of the CAD

We used a retrospective study design based on images (retinograms and OCT) and clinical data (visual acuity) randomly extracted from the clinical charts and OCT records from a university-based retina specialty clinic at Tenerife (Canary Islands, Spain). From March to August 2010, 50 consecutive nAMD patients proposed for intravitreal anti-vascular endothelial growth factor (VEGF) therapy after a complete ophthalmic examination or with a disciform retinal scar were considered for the study. Patients were eligible for inclusion in the study if they were older than 50 years and had a previous diagnosis of nAMD (visual acuity+retinogram+OCT). Patients were excluded if they had history of diabetic retinopathy, presence of inflammatory ocular disease or presence of any other macular abnormality such as macular pucker, macular degeneration, retinal vein occlusion or cystoid macular oedema.

Normal OCT images were obtained from a group of 50 healthy subjects randomly recruited from the administrative

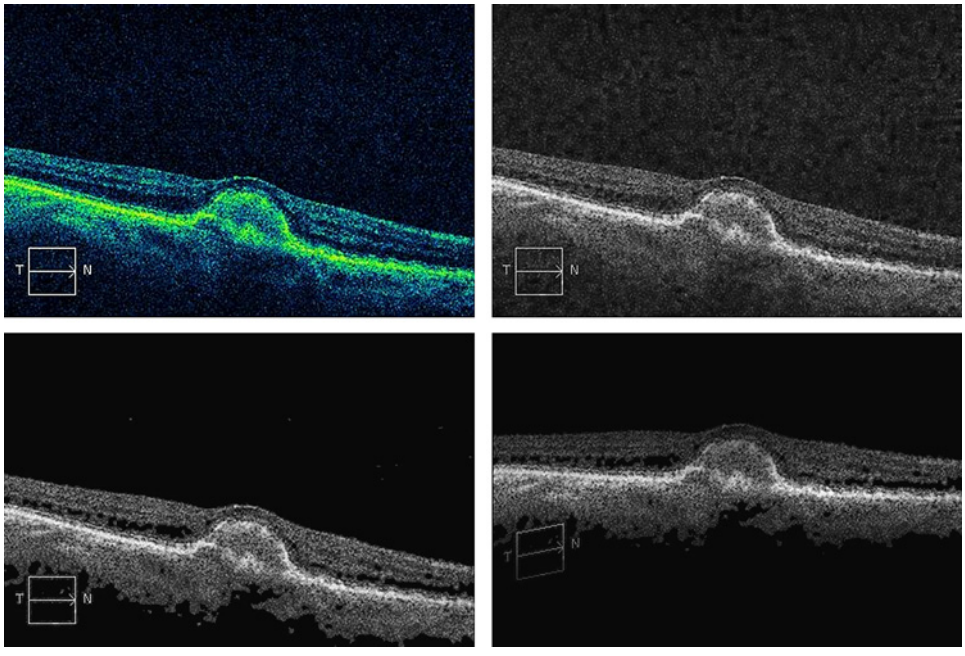

Figure 1 These images correspond to the registration process: source (top left), reflectivity (top right), noise removed (bottom left) and normalised (bottom right). Reflectivity values are computed from the hue–saturation–value (HSV) values of the original image: the warmer the colour, the higher the reflectivity. Then, in order to remove background noise in the vitreous region, pixel values are set to zero if the average reflectivity of a squared window around them is lower than the average reflectivity of the whole image. Tissue deformation and translation is finally modelled and corrected by finding the quadratic Bézier curve that best fits high reflective pixels and finally remapping pixel values to a space where the Bézier curve forms a straight line.

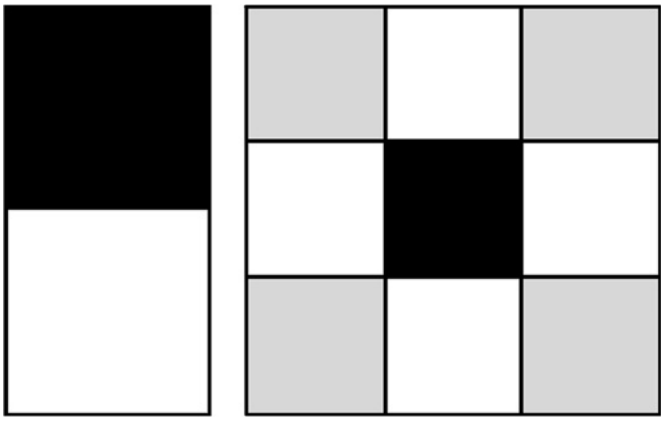

Figure 2 When applied to each A-scan to detect each structure, particle swarm optimisation optimises a certain function that can be explained in terms of Haar-like features. Small analysis windows are considered, summing reflectivity values and evaluating specific functions for each structure. The inner limiting membrane particle fitness function, for example, returns higher values when the top half of the analysis window is darker than the lower half, so its Haar feature looks like that shown in the left image of this figure. Voids are more complex, being a low reflectivity region surrounded by high reflectivity regions in a cross shape, as shown in the right image of this figure, where grey regions are ignored).

services of the hospital and from the general population. For technical assessment purposes two OCT images (horizontal and vertically centred in the fovea) were evaluated from every individual, accounting for a total of 100 images for each group. Only one eye per individual was assessed. Each image was considered independently.

Baseline demographic, medical and ophthalmological data were obtained through retrospective chart review, including age, sex and medical background (table 1). Patients' personal information was masked by the use of a numeric code.

Both normal and AMD OCT images were randomly selected, masked and mixed by an independent researcher from the Health Technology Assessment Unit of the Government of the Canary Islands, before classification by an expert in retina from the University Hospital of Nuestra Señora de la Candelaria (HUNSC) and the CAD. Every image was classified as normal (healthy) or abnormal (probably unhealthy) for screening purposes. Due to this basic categorical classification it was not possible to estimate the area under the receiver operating characteristic curve as measure of diagnostic validity. Operating indicators of technical validity were restricted to estimations of sensitivity, specificity, positive predictive value (PPV) and negative predictive value (NPV). All OCT studies were performed on a Stratus or Cirrus system (Zeiss Meditec, Dublin, California, USA). We used radial lines or macular cube protocols depending on the system for image acquisition. The retinal border detection algorithm contained in the commercial Stratus OCT software was used. Images were exported for CAD analyses by means of the own software of Zeiss Meditec included in the system.

Table 1 Baseline main characteristics of the sample

	Individual with normal OCT images	nAMD patients	p Value
Sex: male, n (%)	18 (40)	15 (30)	0.523*
Age, mean (SD)	61.2 (13.8)	74.8 (7.6)	<0.001†‡
Hypertension, n (%)	26 (52)	32 (64)	0.224*
Diabetes mellitus, n (%)	12 (24)	12 (24)	0.999*
Dyslipidaemia, n (%)	20 (40)	33 (66)	0.009*‡
Smoking, n (%)	11 (22)	15 (3)	0.362*

*χ^2.
†t test.
‡Significant p values.
nAMD, neovascular age-related macular degeneration; OCT, optical coherence tomography.

RESULTS

The baseline characteristics of the sample population (healthy and nAMD patients) are shown in table 1. nAMD patients were significantly older and had a higher prevalence of dyslipidaemia than the sample of healthy individuals.

The normalisation algorithm was able to quantify image information while preserving tissue reflectivity by working in the perceptually uniform HSV colour space. The use of quadratic Bezier curves both describes and allows the correction of geometric deformations due to registration errors.

Particle swarm optimisation combined with Haar-like features was suitable to reveal structural features (main tissue clusters, retinal pigment epithelium (RPE) and inner limiting membrane layers, hole-like structures (HLS) and foveola region) in both normal and abnormal OCT images. In the former, detected structures keep spatial consistency. Abnormal images are usually scattered vertically and spatial coherence may not be maintained (figure 3). The use of decision trees allowed the characterisation of normal and abnormal images by means of feature vectors obtained from descriptive statistics of detected structures.

For the technical validation of the CAD we used a total of 200 OCT images (two per individual) (50 normal and 50 abnormal), offering a sensitivity value of 96% (95% CI 92 to 100); a specificity of 92% (95% CI 87 to 97); a positive predictive value of 92% (95% CI 87 to 97), and negative predictive value of 96% (95% CI 92 to 100), with a positive and negative probability coefficient of 12 (95% CI 6.17 to 23) and 0.04 (95% CI 0.02 to 0.11), respectively.

DISCUSSION

Cost-effective early detection and treatment of prevalent eye diseases such as AMD can have a significant impact on reducing the incidence of vision loss and blindness. Detection of AMD in asymptomatic stages is especially important now that effective preventive[2] and therapeutic[3] interventions are available. Unfortunately, most people do not undergo routine eye examinations due to the lack of symptoms and/or shortage of ophthalmologic resources.

New laser-based imaging platforms such as OCT and CAD methods generate high-quality digital data that have the potential to enhance the ability of the clinician to effectively screen large, at-risk populations for specific diseases.

In this article, an unassisted CAD solution for automated analysis and classification of OCT images is proposed. Contrary to previously reported literature on CAD development from OCT images,[11–14] our solution does not focus exclusively on the segmentation of retinal layers but on the classification of images in two categories (normal–abnormal). Most previously reported solutions[11–13] rely on the extraction of retinal layer thickness and layer boundaries, but nothing is said about their performance for abnormal images where boundaries may disappear. The proposed solution is able to deal with both normal and heavily deformed macular tissues. Decision trees are able to elucidate the most important variables in a set of feature vectors, discarding those that are uninformative. This allows the creation of feature vectors that may contain redundant information. Once trained, decision trees are able to classify new images (ie, their feature vectors) in a computationally inexpensive process. Moreover, they are also able to explain how they reached

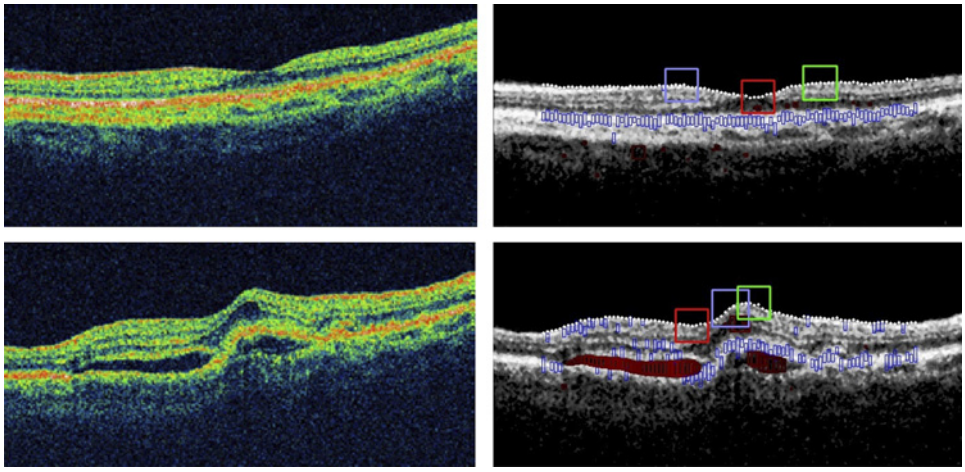

Figure 3 Top row: normal image. Bottom row: abnormal image. The red square shows the position of the foveal region. Blue and green squares show left and right clivus location, respectively (wrongly placed in the abnormal image). Proposed inner limiting membrane, retinal pigment epithelium and hole-like structures are marked with white diamonds, blue rectangles and red rectangles, respectively.

a certain decision, becoming a useful aid as a screening tool in a first diagnostic stage.

Although there are data on the adequate sensitivity and low-moderate specificity of Stratus OCT compared with fluorescein angiography to monitor choroidal neovascularisation after photodynamic therapy,[22] the requirements for screening for AMD in the general population using OCT images have been insufficiently assessed.[15] The values reached by OCTAL for sensitivity (96%), specificity (92%), PPV (92%) and NPV (96%) to screen for AMD seem promising. Although the differences observed between population samples (nAMD patients and healthy individuals) due to age and the prevalence of dyslipidaemia are not relevant at this stage of CAD design and technical validation, they should be carefully considered and controlled for in the planned next stage of clinical validation.

Public national health systems have defined a set of criteria to inform the suitability of a screening programme: relevance of the health problem; known natural history and epidemiology; availability of a simple, safe, precise, cost-effective screening test, acceptable for the target population; availability of a valid diagnostic test; and effective treatment.[23] Although increasing evidence seems to support screening interventions for nAMD, studies undertaking research on AMD screening tools have had difficulties in assessing simple and effective tools to be used at the community level.[2 24 25] One relevant problem for any screening test for AMD is the limitation to detect recent disease onset or progression.

Once OCTAL has proven its technical validity, the next step will be the assessment of the clinical validity and utility. Theoretically the application of computer-based image analysis has the potential to facilitate early recognition and management of AMD by increasing throughput, reducing costs, and assisting or potentially automating diagnostic capabilities if they can be effectively integrated into a tele-medical network delivery system. These objectives will need to be assessed before modelling and assessing the organisational issues of an AMD screening programme. The low rates of diagnosis of AMD (only 30–45% of AMD patients are diagnosed) highlight the potential value of this CAD.

A literature search on electronic databases of biomedical research focused on automated screening of AMD based on OCT images, performed in February 2009 and repeated in July 2010, retrieved only one report of interest, assessing the value of CAD for the automated diagnosis of clinically significant macular oedema, but none specifically focused on AMD.[15]

At this stage of OCTAL development, the system allows the rough detection of certain structures and features to characterise normal and abnormal images. Future system iterations and improvements should focus on the post-processing of available information (eg, retinal pigment epithelium (RPE) points and tissue holes) to improve image classification.

This validation study demonstrates that OCTAL is a new CAD with technical validity that needs to be assessed in a clinical context to test its clinical validity and utility. In this early stage of OCTAL development, adequate levels of sensitivity and specificity to distinguish between normal and abnormal nAMD OCT images have been obtained. These outcomes allow us to proceed with its clinical validation and the subsequent cost-effectiveness assessment before recommendations can be made for population-screening purposes.

Funding This research study was financed by the Health Institute Carlos III (Fondo de Investigaciones Sanitarias File No PS09/01308).

Competing interests None to declare.

Patient consent Obtained.

Ethics approval Ethics Committee of the University Hospital of Nuestra Señora de la Candelaria (HUNSC) of Tenerife, Canary Islands (Spain). The study was carried out in accordance with the Declaration of Helsinki.

Contributors PSA: conception and organization of the research project and writing of the first draft of the manuscript and approval the final version to be published. RA: conception and execution of the research project and drafting the article and approval the final version to be published. LAC: design and programming of the computer-aided diagnostic software, drafting the article and approval the final version to be published. CGA: design of the computer-aided diagnostic software, revision of the manuscript and approval the final version to be published. YRF: validation of computer-aided diagnostic software, statistical analysis and interpretation of data and revision of the manuscript, and approval the final version to be published. FGU: execution of the research project, review and critique of the manuscript and approval the final version to be published. JN: execution of the research project, review and critique of the manuscript and approval the final version to be published.

Provenance and peer review Not commissioned; externally peer reviewed.

REFERENCES

1. **van Leeuwen R,** Klaver CC, Vingerling JR, *et al*. Epidemiology of age-related maculopathy: a review. *Eur J Epidemiol* 2003;**18**:845–54.
2. **Age-Related Eye Disease Study Research Group.** A randomized, placebo-controlled, clinical trial of high-dose supplementation with vitamins C and E, beta-carotene, and zinc for age-related macular degeneration and vision loss: AREDS report no. 8. *Arch Ophthalmol* 2001;**119**:1417–36.
3. **Colquitt JL,** Jones J, Tan SC, *et al*. Ranibizumab and pegaptanib for the treatment of age-related macular degeneration: a systematic review and economic evaluation. *Health Technol Assess* 2008;**12**:iii-iv, ix–201.
4. **Zimmer-Galler IE,** Zeimer R. Feasibility of screening for high-risk age-related macular degeneration with an internet-based automated fundus camera. *Ophthalmic Surg Lasers Imaging* 2005;**36**:228–36.
5. **Karnon J,** Czoski-Murray C, Smith K, *et al*. A preliminary model-based assessment of the cost-utility of a screening programme for early age-related macular degeneration. *Health Technol Assess* 2008;**12**:iii-iv, ix-124.
6. **Doi K.** Computer-aided diagnosis in medical imaging: historical review, current status and future potential. *Comput Med Imaging Graph* 2007;**31**:198–211.

7. **Bouhaimed M,** Gibbins R, Owens D. Automated detection of diabetic retinopathy: results of a screening study. *Diabetes Technol Ther* 2008;**10**:142—8.
8. **Cabrera Fernández D,** Salinas HM, Puliafito CA. Automated detection of retinal layer structures on optical coherence tomography images. *Opt Express* 2005;**13**:10200—16.
9. **Larsen M,** Gondolf T, Godt J, *et al*. Assessment of automated screening for treatment-requiring diabetic retinopathy. *Curr Eye Res* 2007;**32**:331—6.
10. **Keane PA,** Liakopoulos S, Ongchin SC, *et al*. Quantitative analysis of OCT after treatment with ranibizumab for neovascular age-related macular degeneration. *Invest Ophthalmol Vis Sci* 2008;**49**:3115—20.
11. **Rossant F,** Ghorbel I, Bloch I. Automated segmentation of retinal layers in OCT imaging and derived ophthalmic measures. In: *Proceedings of the Sixth IEEE international Conference on Symposium on Biomedical Imaging: From Nano To Macro (Boston, Massachusetts, USA, June 2009)*. Piscataway, NJ: IEEE Press: 1370—3.
12. **Baroni M,** Diciotti S, Evangelisti A, *et al*. Texture classification of retinal layers in optical coherence tomography. In: Jarm T, Kramar P, Zupanic A, eds. *11th Mediterranean Conference on Medical and Biomedical Engineering and Computing*. Berlin Heidelberg: Springer, 2007:847—50.
13. **Bagci AM,** Shahidi M, Ansari R, *et al*. Thickness profiles of retinal layers by optical coherence tomography image segmentation. *Am J Ophthalmol* 2008;**146**:679—87.
14. **Fuller A,** Zawadzki R, Choi S, *et al*. Segmentation of three-dimensional retinal image data. *IEEE Trans Vis Comput Graph* 2007;**13**:1719—26.
15. **Sadda SR,** Tan O, Walsh AC, *et al*. Automated detection of clinically significant macular edema by grid scanning optical coherence tomography. *Ophthalmology* 2006;**113**:1187.
16. **Viola P,** Jones M. Rapid object detection using a Boosted Cascade of simple features. In: Proceedings of the 2001 IEEE international Conference on Symposium on Biomedical Imaging: Computer Vision and Pattern Recognition(Kauai Marriott, Hawaii, USA, December 2001). Piscataway, NJ: IEEE Press, **1**:511—18.
17. **Quinlan JR.** *C4.5: Programs for Machine Learning*. Massachusetts: Morgan Kaufmann Publishers, 1993.
18. **Hall M,** Frank E, Holmes G, *et al*. The WEKA data mining software: An update. *SIGKDD Explorations* 2009;**11**:10—18.
19. **Omran MG,** Engelbrecht AP, Salman A. A color image quantization algorithm based on particle swarm optimization. *J informatica* 2005;**29**:261—9.
20. **Eriksson U,** Alm A. Macular thickness decreases with age in normal eyes: a study on the macular thickness map protocol in the Stratus OCT. *Br J Ophthalmol* 2009;**93**:1448—52.
21. **Picard RR,** Cook RD. Cross-validation of regression models. *J Amer Statist Assoc* 1984;**79**:575—83.
22. **Keane PA,** Liakopoulos S, Walsh AC, *et al*. Limits of the retinal-mapping program in age-related macular degeneration. *Br J Ophthalmol* 2009;**93**:274—5.
23. **National Screening Committee.** *NSC Criteria for Appraising the Viability, Effectiveness and Appropriateness of a Screening Programme*. http://www.nsc.nhs.uk/pdfs/Criteria.pdf (accessed 5 Jul 2010).
24. **van Leeuwen R,** Chakravarthy U, Vingerling JR, *et al*. Grading of age-related maculopathy for epidemiological studies: is digital imaging as good as 35 mm film? *Ophthalmology* 2003;**110**:1540—4.
25. **Schmitt NJ,** Grover DA, Feldon SE. The Eger macular stressometer: pilot study. *Am J Ophthalmol* 2003;**136**:314—17.